An exponentially fitted enthalpy control volume algorithm for coupled fluid flow and heat transfer

Y.H. Wu* B. Wiwatanapataphee† R. Collinson*
G.Zhang*

(Received 7 August 2000)

Abstract

This paper develops an efficient numerical method for solving the coupled fluid flow and heat transfer with solidification problem. The

*School of Mathematics & Statistics, Curtin University of Technology, Perth, WA 6845, Australia. mailto:yhwu@cs.curtin.edu.au

†Department of Mathematics, Mahidol University, Thailand.

governing equations are the continuity equation, the Navier-Stokes equations and the convection-diffusion equation with a source term due to phase change. Fluid flow in the mushy region is modeled on the basis of Darcy's law for porous media and the solidification process is simulated using a single domain approach via the use of an enthalpy scheme for the convection-diffusion equation. The formulation of the numerical method is cast into the framework of the Petrov-Galerkin finite element method with a step test function across the control volume and locally constant approximation to the fluxes of heat and fluid. The formulation leads to the derivation of exponential interpolating functions for the control volume. The use of the exponentially fitted control volume improves the accuracy of results especially for problems with sharp interior or boundary layers such as the solution around the solidification front. The method is then illustrated through a numerical example.

Contents

1 Governing equations

Consider an incompressible homogeneous fluid contained in a domain Ω with boundary $\partial\Omega$. Let $\mathbf{u}(\mathbf{x},t)$ be the velocity field, $p(\mathbf{x},t) = \frac{\overline{p}(\mathbf{x},t)}{\rho} - \mathbf{F}.\mathbf{x}$ with $\overline{p}$ and ρ being the fluid pressure and density and $\mathbf{F}$ body free, and $T(\mathbf{x},t)$ the temperature field. Then the field equations governing the fluid flow, heat transfer and solidification process in Ω are the continuity equation, the Navier-Stokes equations and the convection diffusion equation, namely

$$\nabla \cdot \mathbf{v} = 0, \tag{1}$$

$$-\nabla \cdot (\frac{1}{R_e}\nabla\mathbf{v} - \mathbf{v}\mathbf{v} - pI) = \mathbf{F}(\mathbf{v},\mathbf{x},t), \tag{2}$$

$$\nabla \cdot (\mathbf{v}T - \alpha\nabla T) = Q, \tag{3}$$

where $R_e > 0$ denotes the Reynolds number, α represents the diffusivity of fluid, $\mathbf{F}(\mathbf{v},\mathbf{x},t)$ is the forcing function which is proportional to the velocity of the liquid relative to the mushy region and is given by

$$\mathbf{F}(\mathbf{v},\mathbf{x},t) = \frac{\mu}{\rho\kappa}(\mathbf{v} - \mathbf{v}_m), \tag{4}$$

where μ and $\mathbf{v}_m$ are respectively the viscosity of the fluid and the velocity of the mushy region (assumed constant), κ denotes the permeability of fluid

defined by [1, 14],

$$\kappa = \frac{f(T)^3}{C(1-f(T)^2)}\,. \tag{5}$$

The liquid fraction $f(T)$ is a function of temperature, varying from zero in the solidified region to one in the liquid region. From (1)–(5), it is obvious that for the solidified region, equations (1) and (2) reduce to $\mathbf{v} = \mathbf{v}_m$. While for the liquid region, $\mathbf{F} \equiv \mathbf{0}$ and equation (2) represents the usual Navier-Stokes equations for incompressible Newtonian fluid. The source term Q arises from the release of latent heat due to phase change and is zero everywhere except in the mushy region where

$$Q = \frac{L}{c}[\nabla \cdot (\mathbf{v}f)] \ , \tag{6}$$

in which L and c denote the latent heat and specific heat of liquid fluid.

For two-dimensional problems, once the function $f(T)$ is known, equations (1)–(3) constitute a systems of four equations in terms of four unknowns u, v, p and T. In this paper, we will study the solution of this system of equations subjected to the following type of boundary conditions

$$\mathbf{v} = \overline{\mathbf{v}} \quad \text{on} \quad \partial\Omega\,, \tag{7}$$

$$T = \overline{T} \quad \text{on} \quad \partial\Omega_1\,, \tag{8}$$

$$-k\frac{\partial T}{\partial n} = h_\infty(T - T_\infty) \quad \text{on} \quad \partial\Omega_2\,, \tag{9}$$

where $\partial\Omega_1 \cup \partial\Omega_2 = \partial\Omega$, k and h_∞ are respectively the conductivity of fluid and the surface heat transfer coefficient, $\overline{\mathbf{v}}, \overline{T}$ and T_∞ are known functions or constants.

It is well known that when the Reynolds number is large, the solutions of the coupled transport problems display sharp boundary layers so that classical methods may lead to unbounded spatial oscillations and fail to yield any useful solutions. To overcome this problem, various Petrov-Galerkin methods such as the upwind type methods [2, 3, 5, 9] and the streamline diffusion type methods [10, 13] have been proposed. However, it has been found that the upwind schemes may also result in inaccurate solutions. A promising technique is the exponentially fitted finite control volume method, which has been developed to solve the nonlinear convection-diffusion equation [17] and the Navier-Stokes equations with stream function and vorticity variable as primary variables satisfactorily [12]. In this study, we develop and test a control volume procedure for the solution of the coupled fluid flow-heat transfer problem with velocity and temperature as primary variables within the framework of the Petrov-Galerkin method. In the following section, we present the Petrov-Galerkin finite element formulation for the problem. In Section 3, we apply the method to study the coupled heat transfer and fluid flow in an industrial process—the continuous steel casting process.

2 Enthalpy control volume formulation

To solve the boundary value problem in Section 1, the continuity requirement (1) is weakened and replaced by

$$\nabla \cdot \mathbf{v} = -\delta p, \tag{10}$$

where δ is a small positive number. Thus, the variational statement corresponding to the boundary value problem under consideration is the following variational boundary value problem,

VBVP: Find $\mathbf{v} \in [H^1(\Omega)]^2$, $p \in H^1(\Omega)$ and $T \in H^1(\Omega)$ such that for all $w \in H_0^1(\Omega)$, equations (7)–(8) are satisfied and

$$(\nabla \cdot \mathbf{v}, w) = (-\delta p, w), \tag{11}$$

$$-(\nabla \cdot (\frac{1}{R_e}\nabla \mathbf{v} - \mathbf{v}\mathbf{v} - p\mathbf{I}), w) = (\mathbf{F}, w), \tag{12}$$

$$(\nabla \cdot (\mathbf{v}T - \alpha \nabla T), w) = (Q, w), \tag{13}$$

where $(\cdot, \cdot)$ denotes the inner product on $L^2(\Omega)$, $H^1(\Omega)$ is the Sobolev space $W^{1,2}(\Omega)$ with norm $\| \cdot \|_{1,2,\Omega}$,

$$H_0^1(\Omega) = \{ v \in H^1(\Omega) \mid v = 0 \text{ on Dirichlet boundary } \}.$$

To solve the VBVP, we discretize Ω into a finite number of elements Ω_i and construct two finite dimensional subspaces H_a for $\mathbf{v}$, p and T, and H_t for the weighting function w, namely, $\mathbf{v}$, p, T and w are approximated by

$$\begin{aligned} \mathbf{v} \approx \mathbf{v}_h = \sum_{i=1}^{N} \phi_i \mathbf{v}_i, \quad p \approx p_h = \sum_{i=1}^{N} \phi_i p_i, \\ T \approx T_h = \sum_{i=1}^{N} \phi_i T_i, \quad w \approx w_h = \sum_{i=1}^{N} \psi_i w_i, \end{aligned} \tag{14}$$

where ϕ_i and ψ_i are respectively the basis functions of H_a and H_t, namely $H_a = \text{span}(\phi_i)$ and $H_t = \text{span}(\psi_i)$. Thus, the two basic design choices for the numerical approximation are the trial space H_a and the test space H_t. The form of the error distribution over Ω depends on the choice for the basis function ψ_i. To construct a control volume procedure, we choose ψ_i as follows:

$$\psi_i = \begin{cases} 1 & \text{on } \Omega_i \\ 0 & \text{otherwise.} \end{cases} \tag{15}$$

Then from the VBVP, by taking $w \approx w_h = \psi_i$ and using Green's formula and the one point quadrature rule for integral in Ω_i, we have for $i = 1, 2, 3, \ldots, N$,

$$\int_{\partial\Omega_i} \mathbf{v} \cdot \mathbf{n} \, ds = -\delta \, p_i \, |\Omega_i|, \tag{16}$$

$$-\int_{\partial\Omega_i} \left(\frac{1}{R_e}\nabla\mathbf{v} - \mathbf{v}\mathbf{v}\right) \cdot \mathbf{n} \, ds = -\int_{\partial\Omega_i} p\mathbf{I} \cdot \mathbf{n} \, ds + |\Omega_i| \mathbf{F}_i(\mathbf{v}, \mathbf{x}, t), \tag{17}$$

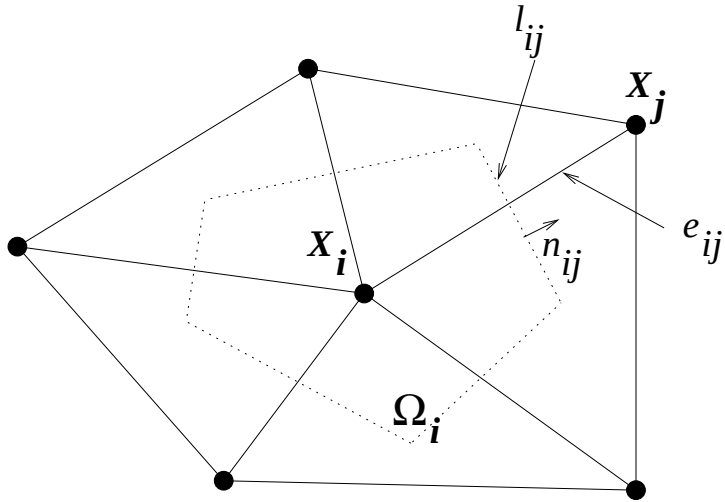

FIGURE 1: Control volume of node X_i

$$-\int_{\partial\Omega_i}(\alpha\nabla T-\mathbf{v}T)\cdot\mathbf{n}\,ds=-\frac{L}{c}\int_{\partial\Omega_i}(\mathbf{v}f)\cdot\mathbf{n}\,ds. \tag{18}$$

Let $\mathcal{X}=\{\mathbf{x}_i \mid i=1,\ldots,N\}$ denote the set of all vertices, I_i denote the index set of the neighbouring nodes of $\mathbf{x}_i$, $\mathbf{n}_{ij}$ be the unit vector pointing from $\mathbf{x}_i$ to $\mathbf{x}_j$, l_{ij} be the part of $\partial\Omega_i$ perpendicular to the unit vector $\mathbf{n}_{ij}$, as shown in Figure 1. Then, equations (16)–(18) become

$$\sum_{j\in I_i}\int_{l_{ij}}\mathbf{v}\cdot\mathbf{n}_{ij}\,ds=-\delta\,|\Omega_i|p_i, \tag{19}$$

$$-\sum_{j\in I_i}\int_{l_{ij}}(\frac{1}{R_e}\nabla\mathbf{v}-\mathbf{vv})\cdot\mathbf{n}_{ij}\,ds=-\sum_{j\in I_i}\int_{l_{ij}}p_i\,\mathbf{I}\cdot\mathbf{n}_{ij}\,ds+|\Omega_i|\mathbf{F}_i(\mathbf{v},\mathbf{x},t), \quad (20)$$

$$-\sum_{j\in I_i}\int_{l_{ij}}(\alpha\nabla T-\mathbf{v}T)\cdot\mathbf{n}_{ij}\,ds=-\frac{L}{c}\sum_{j\in I_i}\int_{l_{ij}}(\mathbf{v}f)\cdot\mathbf{n}_{ij}\,ds. \quad (21)$$

The integral terms in equations (19)–(21) represent the outward fluxes crossing l_{ij}. By approximating the flux across each l_{ij} as a constant and finding the constant in terms of the nodal values of the unknown function at $\mathbf{x}_i$ and $\mathbf{x}_j$, we obtain

$$\sum_{j\in I_i} l_{ij}\mathbf{v}(c)\ \cdot\mathbf{n}_{ij}=-\delta\ |\Omega_i|p_i, \quad (22)$$

$$\begin{aligned}-&\sum_{j\in I_i}\frac{l_{ij}}{R_e|\Omega_i||\mathbf{x}_j-\mathbf{x}_i|}\{B(\xi)\mathbf{v}_j-B(-\xi)\mathbf{v}_i\}\\ =\ &-\sum_{j\in I_i}\frac{l_{ij}}{|\Omega_i|}\,p(c)\mathbf{I}\cdot\mathbf{n}_{ij}+\mathbf{F}_i(\mathbf{v},\mathbf{x},t),\end{aligned} \quad (23)$$

$$-\sum_{j\in I_i}\frac{l_{ij}\alpha}{|\Omega_i||\mathbf{x}_j-\mathbf{x}_i|}\{B(\zeta)T_j-B(-\zeta)T_i\}+\frac{L}{c}\sum_{j\in I_i}\frac{l_{ij}}{|\Omega_i|}(\mathbf{v}_i\mathbf{n}_{ij})f_i=0, \quad (24)$$

where

$$\mathbf{v}(c)=\frac{\mathbf{v}_i+\mathbf{v}_j}{2},$$

$$\xi=R_e(\mathbf{v}_i\cdot\mathbf{n})|\mathbf{x}-\mathbf{x}_i|,\quad \zeta=\frac{1}{\alpha}(\mathbf{v}_i\cdot\mathbf{n})|\mathbf{x}_j-\mathbf{x}_i|,$$

and $B(\xi)$ is the Bernoulli function defined by

$$B(\xi) = \begin{cases} 1 & \xi = 0 \\ \frac{\xi}{e^{\xi}-1} & \xi \neq 0 \end{cases}.$$

For points on the heat flux boundary, using boundary condition (9), equation (1) becomes

$$-\sum_{j\in I_i^*} \frac{l_{ij}\alpha}{|\Omega_i||\mathbf{x}_j - \mathbf{x}_i|}\{B(\zeta)T_j - B(-\zeta)T_i\}$$

$$+\frac{L}{c}\sum_{j\in I_i} \frac{l_{ij}}{|\Omega_i|}(\mathbf{v}_i \cdot \mathbf{n}_{ij})f_i = \frac{\sum_{k=1}^{N_b} l_{ik}}{\rho c|\Omega_i|}\{h_\infty(T_\infty - T_i)\},$$

where I_i^* is the index set of the neighbouring nodes of $\mathbf{x}_i$ which are not on the heat flux boundary, l_{ik} and N_b denote respectively the length of the line segment and the number of line segments on the heat flux boundary of $\partial\Omega_i$. By assembling the element equations over all control volumes, we obtain

$$\mathbf{P} = \mathbf{C}(\mathbf{U}), \tag{25}$$

$$\mathbf{K}_u\mathbf{U} = \mathbf{C}'\mathbf{P} + \mathbf{F}, \tag{26}$$

$$\mathbf{K}_T\mathbf{T} + \mathbf{A}\boldsymbol{f} = \mathbf{F}_b, \tag{27}$$

where $\mathbf{U}$ and $\mathbf{T}$ are global vectors with U_i and T_i representing respectively

the velocity and temperature at node i, and all coefficient matrices refer to global matrices. Matrices $\mathbf{K}_u$ and $\mathbf{K}_T$ correspond to the convection-diffusion term; Matrix $\mathbf{A}$ corresponds to the convection term of latent heat; matrix $\mathbf{C}'$ corresponds to the pressure term; vector $\mathbf{C(U)}$ corresponds to the penalty term; vector $\mathbf{P}$ denotes the pressure field; vectors $\mathbf{F}$ and $\mathbf{F}_b$ provide forcing functions for the system.

3 A numerical example

As an application example, we study the coupled fluid flow - heat transfer in the continuous steel casting process. Various numerical studies have been conducted to analyse the heat transfer and fluid flow phenomena in the continuous casting process [4, 6, 7, 8, 11, 15, 16]. However, only few studies solve the coupled problem. In this paper, we use the method presented to solve the coupled problem. Figure 2 shows the fluid flow region under consideration. Molten steel is poured continuously into a water cooled mould through the nozzle as shown. Intensive cooling in the rigid heat flux boundary causes a thin solidified steel shell to form around the edge of the steel. The steel shell is then withdrawn from the bottom of the mould at a constant speed U_{cast}. The depth of the caster is $z_m = 0.8m$, half-width is $0.875m$. The submergence depth of the nozzle inlet is $230mm$. The nozzle port is rectangular with a height of $76mm$, a width of $55mm$ and an angle of 15^oC downward. The solution is limited to a depth of 8 meters below the meniscus. With the

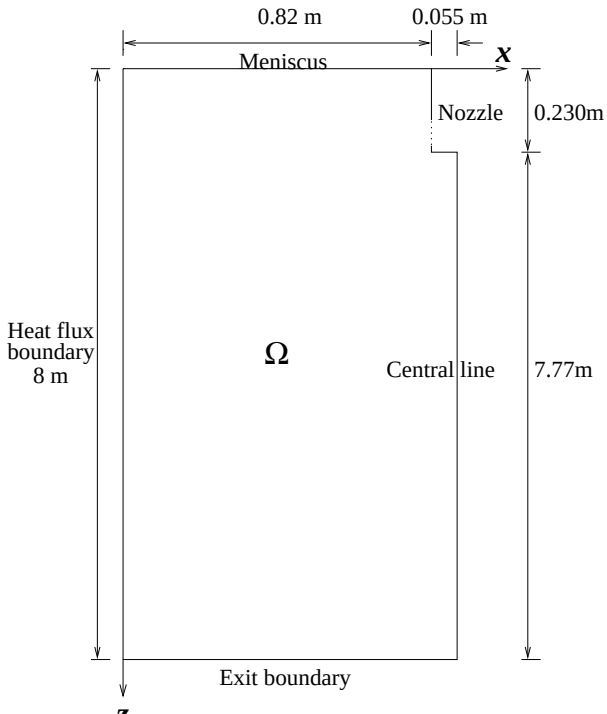

FIGURE 2: Computation region and coordinate system

computer resources available and a mesh-sensitivity study, the finite volume mesh constructed for the present study consists of 1080 nodes. The basic parameters are as follow: $T_\infty = 20^o$C, $T_{ext} = 100^o$C, $U_{cast} = 0.022\,$m/s, $\rho = 7800\,$kg/m^3, $\mu = 0.001\,$pa.s, $c = 465\,$J/kg^{o}C, $k = 35\,$W/m^{o}C, $L = 272000\,$J/kg, $h_\infty = 1079\,$W/m^{2o}C, the temperature of molten steel poured into the mould is 1530^oC, the solidification temperature and melting temperature are respectively 1465^oC and 1525^oC.

Figure 3 shows the velocity vectors and temperature contours in the upper part of the solution domain. It shows how molten steel leaves the nozzle as a strong hot jet. The velocity of the hot jet decays to about 30% of the inlet value while it travels only half way across a mould wall. When the jet hits the mould wall, it splits to flow both upward and downward and then creates a small upper recirculation zone and a big lower recirculation zone. As the steel travels along the mould wall, it moves at the casting speed when its temperature is below the solidification temperature (1465^oC) so that there is an abrupt change in velocity on the solid-liquid interface in the upper part of the casting region. Eventually, the velocity profile becomes parallel further down the strand. In this figure, the temperature profiles clearly outline the path of the hot steel and shows how the fluid carries heat with it. The temperature of the jet drops 2/10 of its superheat while it travels only half way across the mould. It indicates that the jet does not cool down much in the liquid pool. Figure 4 shows the growth of the solidified steel shell in the mould region ($0 \leq z \leq 0.8$m). It is noted that solidification speed decreases with depth.

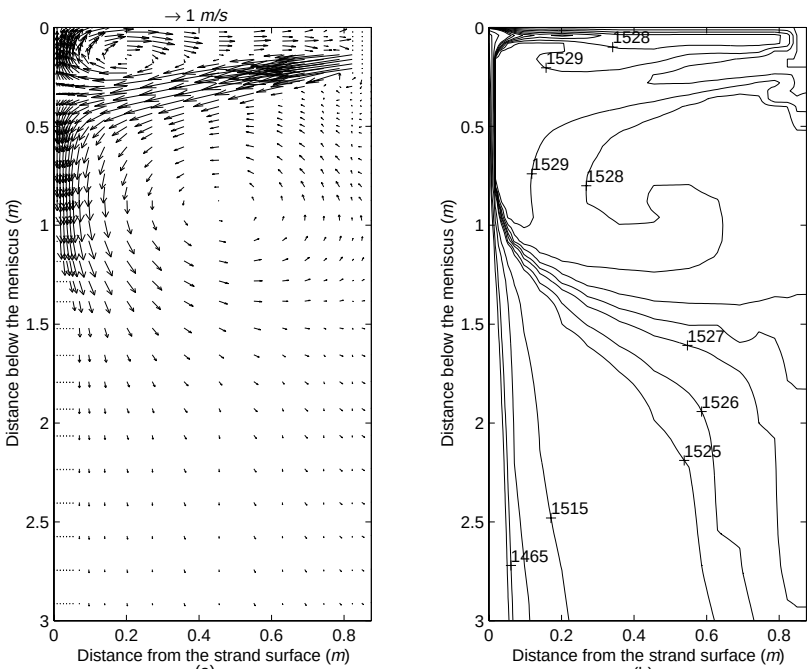

FIGURE 3: Velocity vectors (m/s) and temperature contours (^{o}C)

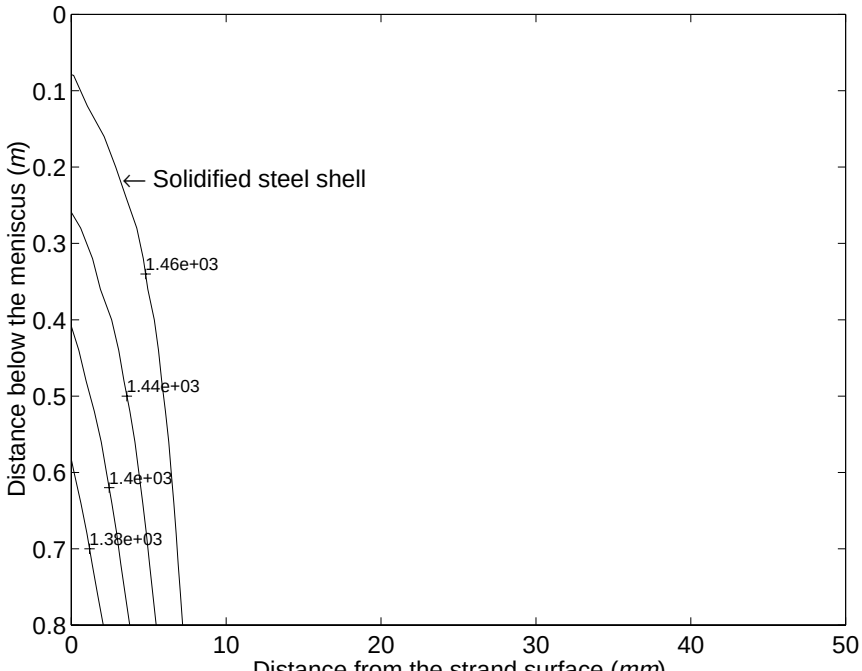

FIGURE 4: Temperature profile (^{o}C) in the solidified region

4 Conclusions

An efficient control volume method has been developed within the framework of the Petrov-Galerkin finite element method for solving the coupled fluid flow-heat transfer with solidification problem. The advantage of the method is that it combines the intrinsic geometric flexibility of finite element methods together with the desirable, direct physical invocation of a conservation principle to clearly identified and delineated control volumes comprising the domain. The use of the exponential interpolation functions enable the scheme to capture the rapid change of temperature in the solidification region, and the rapid change of fluid velocity near the solid-fluid interface. The numerical investigation shows that the method developed is robust in capturing the characteristics of fluid flow and heat transfer in the continuous steel casting process.

References

[1] M.R. Aboutalebi, M. Hasan, and R.I.L. Guthrie. Coupled turbulent flow, heat and solute transport in continuous casting processes. *Metallurgical and Materials Transactions B*, 26B:731–744, 1993. C1583

[2] R.E. Bank, J.F. Bürgler, W. Fitchner, and R.K. Smith. Some upwinding techniques for finite element approximations of convections-diffusion equations. *Numer. Math.,* 58:185–202, 1990. C1584

[3] I. Christie, D.F. Griffiths, A.R. Mitchell, and O.C. Zienkiewicz. Finite element methods for second order differential equations with significant first derivatives. *Int. J. Num. Meth. Engng.*, 10:1389–1396, 1976. C1584

[4] P.J. Flint. A three-dimensional finite difference model of heat transfer, fluid flow and solidification in the continuous slab caster. *Steelmaking Conference Proceeding,* 481–490, 1990. C1590

[5] J.C. Heinrich, P.S. Huyakorn, A.R. Mitchell, and O.C. Zienkiewicz. An upwind finite element scheme for two-dimensional convective transport equations. *Int. J. Num. Meth. Engng.,* 11:131–143, 1997. C1584

[6] J.M. Hill and Y.H. Wu. On a nonlinear Stefan problem arising in the continuous casting of steel. *Acta Mechanica,* 107:183–198, 1994. C1590

[7] Y. Ho and W.S. Hwang. The analysis of molten steel flow in billet continuous casting mold. *ISIJ International,* 36:(8)1030–1035, 1996 . C1590

[8] X. Huang, B. Thomas, and F. Najjar. Modeling superheat removal during continuous casting of steel slabs. *Metallurgical and Materials Transactions B*, 23B:339–356, 1990. C1590

[9] J.T.R. Hughes and A.N. Brooks. A multidimensional upwind scheme with no crosswind diffusion. In J.T.R. Hughes, editor, *Finite Element Methods for Convection Dominated Flows,* AMD Vol. **34**, Amer. Soc. of Mech. Eng., New York, 1979. C1584

[10] C. Johnson. Streamline diffusion methods for problems in fluids. In R.H. Gallagher *et al.*, editors, *Finite Elements in Fluids*, vol VI, pages 251–261, London, 1986. John Wiley and Sons. C1584

[11] E. Latinen and P. Neittaanmaki. On numerical simulation of the continuous casting process. *J. Eng. Math.,* 22:335–354, 1988. C1590

[12] J.J.H. Miller and S. Wang. An exponetiallly fitted finite volume method for the numerical solution of 2-D incompressible flow problems. *J. Comp. Phys.*, 115(1):56–64, 1994. C1584

[13] K.W. Morton. *Numerical Solution of Convection-Diffusion Problems.* Chapman and Hall, London, 1995. C1584

[14] M.P. Reddy and J.N. Reddy. Numerical simulation for forming processes using a coupled fluid flow and heat transfer model. *International Journal of Numerical Methods for Engineering*, 35:807–833, 1992. C1583

[15] B.G. Thomas, L.J. Mika, and F.M. Najjar. Simulation of fluid flow inside a continuous slab-casting machine. *Metallurgical Transactions B,* 21B:387–400, 1990. C1590

[16] Y.H. Wu, J.M. Hill, and P.H. Flint. A noval finite element method for heat transfer in the continuous caster. *Australian Mathematics Society Series B,* 35:263–288, 1994. C1590

[17] Y.H. Wu, J.B. Song, and J.W. Tian. A control volume procedure for nonlinear convection-diffusion equations. In J. Noyer, M. Teubner, and A. Gill, editors, *Computational Techniques and Applications*, pages 751–758, Singapore 1998. World Scientific Publisher. C1584